Agricultural Water Management 216 (2019) 365–378

Contents lists available at ScienceDirect

Agricultural Water Management

journal homepage: www.elsevier.com/locate/agwat

Impacts of climatic variables on reference evapotranspiration during growing season in Southwest China

Shouzheng Jiang[a], Chuan Liang[a], Ningbo Cui[a,*], Lu Zhao[a], Taisheng Du[b], Xiaotao Hu[c], Yu Feng[a], Jing Guan[a], Yi Feng[a]

[a] State Key Laboratory of Hydraulics and Mountain River Engineering & College of Water Resource and Hydropower, Sichuan University, Chengdu, China
[b] Center for Agricultural Water Research in China, China Agricultural University, Beijing, China
[c] Institute of Water-Saving Agriculture in Arid Areas of China, Northwest A&F University, Yangling, China

ARTICLE INFO

Keywords:
Reference evapotranspiration (ET_0)
Climatic variables
Sensitivity coefficient
Contribution rate
Southwest China

ABSTRACT

Reference evapotranspiration (ET_0) plays an important role in studies on hydrological cycles and environmental change. In present research, the temporal changing characteristics of climatic variables, as well as growing season ET_0 and attribution analysis of ET_0 trend from 1961 to 2016 were investigated at 99 meteorological stations across the Western-Sichuan Plateau, Sichuan Basin, Yunnan-Guizhou Plateau, and Guangxi Basin in Southwest China (SC). The results showed that the change point for ET_0 series was detected in 1996 by the Cramer's test method. Growing season ET_0 declined significantly ($P < 0.01$) by 10.25mm/decade during 1961–1996, while it increased significantly ($P < 0.05$) during 1997–2016 by 8.12 mm/decade. Maximum temperature (T_{max}) and minimum temperature (T_{min}) exhibited a significant increasing trend during 1961–2016, while relative humidity (RH), wind speed (WS) and sunshine duration hours (SD) showed a significant downward trend in SC. ET_0 was highly sensitive to RH, followed by SD, T_{max}, T_{min} and WS, whilst the sensitivity of ET_0 to climatic variables fluctuated during the growing season. The results of attribution analysis showed that the decline in SD as well as WS allocated the significant decrease in ET_0, offsetting the impact of increased temperature during 1961–1996. However, decreased RH and increased air temperature commonly reversed the trend in ET_0 during 1997–2016 in SC. The contribution rate of each climatic variable exhibited great variations both temporally and spatially due to the differences in geographical location and climatic conditions. The increase in ET_0 will result in higher water consumption for the growth of crops, especially for Western-Sichuan Plateau and Yunnan-Guizhou Plateau, appeared to have experienced a more significant increase ($P < 0.05$) from 1997 to 2016. The results can provide a guideline for the regional agricultural production administration and allocation of water resources in the context of ongoing climate change.

1. Introduction

Reference evapotranspiration (ET_0) is a vital parameter of climatic and environmental change, which is closely link to the meteorological and hydrological cycles (Roderick et al., 2009; Fan et al., 2016). ET_0 is not only an important parameter in water balance and water conversion, but also plays an important role in the energy exchange process in the earth-atmospheric system (Gao et al., 2016; Feng et al., 2018). A thorough understanding of spatiotemporal trends of ET_0 in the context of ongoing climate change is of great significance for the planning of regional agricultural production system and water resources management. Therefore, the study of spatial and temporal changes of ET_0 has attracted much attention as it is the most relevant indicator of hydroclimatic changes and water cycles (Yin et al., 2010; Jhajharia et al., 2012).

Researches have shown that the global surface air temperature has risen by 0.85 °C on average during 1880–2012 (Stocker et al., 2014), and is expected to rise by more than 1.5 °C within one hundred years (Pachauri et al., 2014). One of the projected consequences is that the rising temperature should have increased evaporation requirement, however, both observed pan evaporation and ET_0 were found to have decreasing trends in many regions around the world (Golubev et al., 2001; Moonen et al., 2002; Burn and Hesch, 2007; Zhang et al., 2007; Fan and Thomas, 2013), which is known as the "evaporation paradox" (Peterson et al., 1995; Jhajharia et al., 2012; Roderick et al., 2009; Li et al., 2012; Wang et al., 2017). Some researchers revealed the decline

* Corresponding author at: College of Water Resource and Hydropower, Sichuan University, 610065, Chengdu, China.
E-mail addresses: cuiningbo@scu.edu.cn, cuiningbo@126.com (N. Cui).

https://doi.org/10.1016/j.agwat.2019.02.014
Received 4 September 2018; Received in revised form 25 January 2019; Accepted 9 February 2019
Available online 19 February 2019
0378-3774/

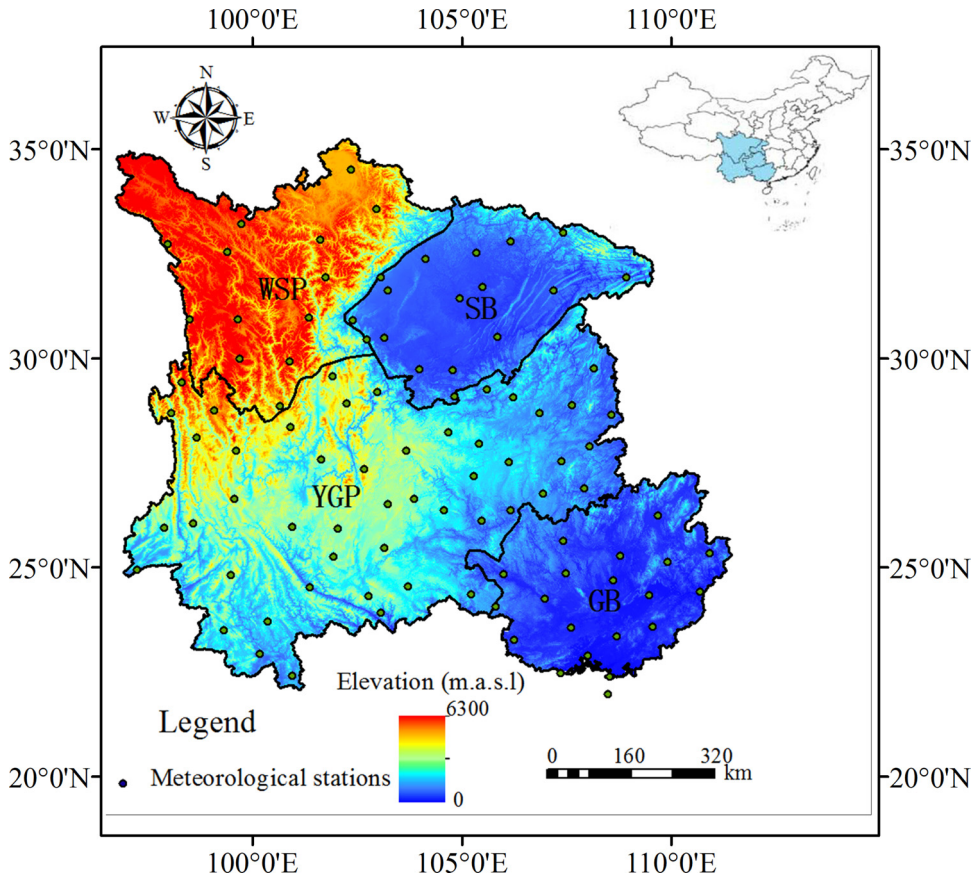

Fig. 1. The distribution of sub-regions and the geographic location of the meteorological stations across Southwest China. WSP: Western-Sichuan Plateau; SB: Sichuan Basin; YGP: Yunnan-Guizhou Plateau; GB: Guangxi Basin.

in sunshine duration resulting from the increasing cloud cover (global dimming) was the dominant cause for the decrease in ET_0 in the wet regions of China, south-eastern Norway, and America over the past 50 years, because it reduced the energy required for ET_0 (Peterson et al., 1995; Stanhill and Cohen, 2001; Grimenes and Thue-Hansen, 2006; Jhajharia et al., 2012; Qian et al., 2015). Meanwhile, other researchers indicted the factor of decreasing wind speed was the foremost climatic variable for the declining ET_0 in Canada (Burn and Hesch, 2007), Iran (Dinpashoh et al., 2011), and arid and semi-arid regions of China (Liu and Zhang, 2013; Wang et al., 2017), which was termed "wind stilling" (McVicar et al., 2012;). Furthermore, humidity and air temperature were also considered to be the main causes for ET_0 variation in India and some regions of China (Qian et al., 2007; Cong et al., 2009; Bandyopadhyay et al., 2009; Zuo et al., 2012). However, they indicated that the variations of ET_0 may not be caused by a single factor, but rather, to an integrated effect of many climatic variables. The explanations given by different researchers seem dissimilar with each other due to the differences in the study areas conducted or different approaches adopted (Hupet and Vanclooster, 2001; Lenhart et al., 2002; Estevez et al., 2009; Fan et al., 2016). Thus, it is important to carry out a regional research for local water resources planning and management.

Although the whole change trend of ET_0 is decreasing in the recent decades from the global perspective, the increasing ET_0 was reported in some areas since 1980s–1990s. Papaioannou et al. (2011) investigated the trend of annual ET_0 from 1950 to 2001 in Greece and discovered it had a declined trend before the early 1980s, conversely, it has begun to increase until 2001. Wang et al. (2017) found that a change appeared in 1982 for the annual ET_0 series in China and wind speed was thought to be the primary influential climatic variables related to the enhanced ET_0. However, Zuo et al. (2012) found that a change point appeared in 1993 for the temporal variability of annual ET_0 series in the Wei River basin of China, and the same phenomenon was also found in Northwest China (Liu and Zhang, 2013). The variation of ET_0 is highly diverse across different regions of China in the content of climate change, it is thus necessary to study the latest change in regional ET_0 and its driving mechanism (McVicar et al., 2012).

Knowledge of the changing characteristics of ET_0, especially the spatial and temporal evolution is the initial step in calculating regional crop evapotranspiration and for irrigation water planning. Probing the effects of climatic variables on ET_0 variation in the growing season, would assist in predicting the variation of ET_0 and providing basic scientific references for agricultural activities, water resources planning and management. The increasing ET_0 was detected in many regions of the world in recent years (Papaioannou et al., 2011; Liu and Zhang, 2013; Li et al., 2016), however, few researchers explore the primary driving factors affecting the growing season ET_0, as well as crop water demand evolutions in Southwest China, which formed the motivation of this research. The objectives of current research were: (1) to detect the change of ET_0 series with the Cramer's test method, and map the spatial distributions of ET_0 and key climatic variables during the growing season (April to September) in the Southwest China before and after the change point using the inverse distance weight interpolation method; (2) to analyze the trends of ET_0 and key climatic variables in the growing season adopting the non-parametric Mann-Kendall test method; (3) to quantify the sensitivity of ET_0 to various climatic variables using the partial derivative sensitivity coefficients method, and further explore their distributions and temporal trends; (4) to determine the key climatic variables and their differences in affecting ET_0 in the growing season with the comparative relative contribution method.

2. Material and methods

2.1. Description of study area and data processing

The study was carried out in Southwest China (SC), located within 20°54′–34°19′N and 91°21′E–112°04′E and with an area of 1.4 million km^2. SC experiences a typical monsoonal climate, controlled by the South Asia monsoon, as well as affected by the East Asia monsoon (Gao et al., 2014), with obvious moisture transfer characteristics of dry and wet season changes. Less water vapor is brought by westerly winds in winter and spring because of the obstruction of Tibetan Plateau, while the monsoonal moisture originates from the Bay of Bengal and the South China Sea in summer and from the western Pacific Ocean in autumn (Feng et al., 2014; Gao et al., 2014). In current study, SC was divided into four subregions based on the terrain features and geographic locations, i.e., (I) Western-Sichuan Plateau (WSP) with altitudes of 4000–4500 m above sea level (m.a.s.l), (II) Sichuan Basin (SB) with altitudes of 300–700 (m.a.s.l), (III) Yunnan-Guizhou Plateau (YGP) with an elevation range of 1800–1900 (m.a.s.l), and (IV) Guangxi Basin (GB) with altitudes of 80–200 (m.a.s.l) (Fig. 1). The elevation of these areas gradually decreases from west to east and from north to south. The mean growing season precipitation of the WSP, the SB, the YGP and the GB are 708 mm, 920 mm, 876 mm and 1209 mm, respectively.

The main data employed in current research were daily meteorological data during 1961–2016, involving minimum air temperature (T_{min},°C), maximum air temperature (T_{max}, °C), mean relative humidity (RH, %), wind speed at 2 m height (WS, m/s) converted from wind speed at 10 m height by using the conversion formula as recommended by Allen et al (Allan et al., 1998), sunshine duration hours (SD, h/d). The meteorological data were collected from 141 national stations, and supplied by the China Meteorological administration (http://data.cma.cn). The used time-series daily meteorological data were long and continuous, the stations with miss daily data less than 1% were selected and filled with data from the nearby stations by the linear regressive method. The homogeneity and stationarity of climatic variables series were examined according to the test method developed by Haktanir and Citakoglu (2014). Finally, 99 stations were selected in this study. Geographic information, including the longitude and elevation of selected stations were obtained as well, and shown in Fig. 1.

2.2. Calculation of reference evapotranspiration

In current study, the Penman-Monteith (P-M) method was adopted to calculate daily reference evapotranspiration. It is physically based with both the energy balance and aerodynamics and was recommended as the sole standard method for ET_0 estimation by FAO in 1998 (Allan et al., 1998). The formula and has been widely used owing to its consistency, reliability and accuracy (Yin et al., 2010; Li et al., 2017; Feng et al., 2017a). The formula is given as follows:

$$ET_0 = \frac{0.408\Delta(R_n - G) + \gamma\frac{900}{T_{mean}+273}u_2(e_s - e_a)}{\Delta + \gamma(1 + 0.34u_2)} \quad (1)$$

where ET_0 is the daily reference evapotranspiration (mm day^{-1}); Δ is the curve slope of the saturation vapor pressure, (KPa °C^{-1}); R_n is the net radiation on the crop surface(MJ m^{-2} day^{-1}); G is the surface soil heat flux density, (MJ m^{-2} day^{-1}), γ is the psychrometric constant (KPa °C^{-1}), T_{mean} is the mean temperature at 2 m height, (°C); u_2 is the wind speed at the height of 2 m, (m s^{-1}); e_s is the saturation pressure (KPa) and e_a is actual water vapor pressure (KPa). The detailed calculation can be found in Allan et al. (1998).

2.3. Trend analysis and mutation test

The rank-based nonparametric Mann-Kendall (MK) test (Shadmani et al., 2012) was utilized to analyze the temporal variation of ET_0 and related climatic variables. Its superiority exists in the ability of detecting the significance of the long time-series trend, no matter the sample series follow a certain type of distribution. (Ye et al., 2014). The MK method has been widely used for the significant test of hydrological and meteorological data (Fan et al., 2016; Liu et al., 2016).

For mutation test, the Cramer's test method was adopted to verify the stability of a sample sequence by comparing the difference between the average of the whole sample sequence and partial sample sequence (Türkeş, 1996; Zhang et al., 2013). The Cramer's test is based on the statistic t_k:

$$t_k = \sqrt{\frac{n(N-2)}{N - n(1+\tau_k^2)}}\cdot\tau_k \quad (2)$$

$$\tau_k = \frac{\bar{x}_k - \bar{x}}{s},\ \bar{x}_k = \frac{1}{n}\sum_{i=k+1}^{k+n} x_i,\ \bar{x} = \frac{1}{N}\sum_{i=1}^{N} x_i \quad (3)$$

where $\bar{x}$, $\bar{x}_k$ represent the average of the whole sample sequence and the average of partial sample sequence, respectively, and s is the overall sample standard deviation. N is the length of the overall sample sequence and n is the length of the selected partial sample sequence. The null hypothesis that there is no mutation is rejected if $|t_k| > t_o$.

2.4. Linear trend

A series $y_1, y_2, \ldots, y_i, \ldots, y_n$ can be represented by the polynomial (Tang et al., 2011; Feng et al., 2017b):

$$y = a_0 + a_1 t + \cdots + a_m t^n \quad (m < n) \quad (4)$$

where y is response variable (i.e. ET_0 or climatic variables); t is the year. The linear trend of a time series can be evaluated by the least square method and can be expressed as a linear regression equation:

$$y_n(t) = Trendv_i \cdot t + a_0 \quad (5)$$

where the slope $Trendv_i$ is the evaluated trend of the variable v_i, and $Trendv_i \times 10$ is called tendency rate, indicating the variation range of variable v_i per decade. Negative value of $Trendv_i$ indicates a decreasing trend, conversely, positive value of $Trendv_i$ indicates an increasing trend.

2.5. Sensitivity and contribution rate analysis

Different variables have different dimensions and ranges of values, making it difficult to contrast the sensitivity via partial derivatives for multi-variable models (Fan et al., 2016). Therefore, the partial derivative is converted into a dimensionless form to facilitate comparison of different climate factors (Gong et al., 2006). Following the P-M formula, ET_0 is the function of five climatic variables (WS, T_{max}, T_{min}, RH, SD), which can be expressed as:

$$ET_0 = f(WS, T_{max}, T_{min}, RH, SD) \quad (6)$$

The sensitivity of ET_0 to climatic variables can be expressed as follows:

$$Sv_i = \lim_{\Delta V_i \to 0}\left(\frac{\Delta ET_0/ET_0}{\Delta v_i/v_i}\right) = \frac{\partial ET_0}{\partial v_i}\cdot\frac{v_i}{ET_0} \quad (7)$$

where v_i is the climate variable, which represents WS, T_{max}, T_{min}, RH or SD in this study, respectively. SV_i represents the sensitivity coefficient of ET_0 to variable v_i, denoting the percentage change in ET_0 transmitted from the percentage change in v_i. If $SV_i > 0$, ET_0 and v_i will increase or decrease simultaneously, otherwise, they have a reverse relation. The larger the $|SV_i|$, the greater the effect of a given variable has on ET_0 variation. The sensitivity coefficient method is more convenient and accurate compared to other sensitivity analysis approaches (Gao et al., 2016). Thus, it has been widely used in evapotranspiration study (Tang et al., 2011; Zhang et al., 2013; Li et al., 2014a; Wang et al., 2017). In

Table 1
Classification of the sensitivity coefficient.

Sensitivity coefficient	Sensitivity levels
$0.00 \le \lvert Sv_i \rvert < 0.05$	Negligible
$0.05 \le \lvert Sv_i \rvert < 0.20$	Medium
$0.20 \le \lvert Sv_i \rvert < 1.00$	High
$\lvert Sv_i \rvert \ge 1.00$	Very high

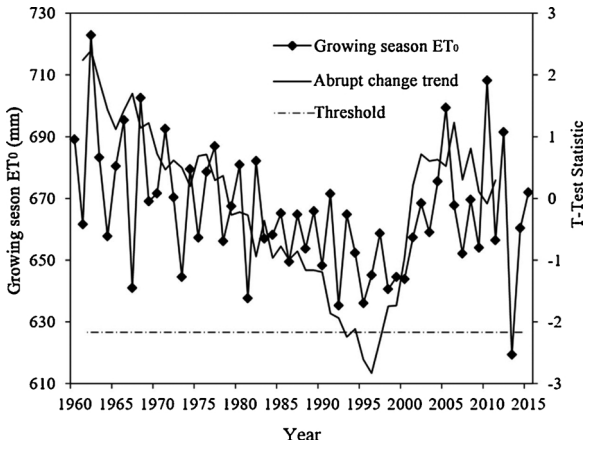

Fig. 2. The trends and abrupt change of growing season ET_0 in Southwest China (SC) during 1961–2016.

this research, sensitivity coefficients were computed on a daily basis for T_{min}, T_{max}, WS, RH, SD. Monthly and growing season averaged sensitivity coefficients were obtained by averaging the corresponding daily sensitivity coefficients. In current study, the sensitivity coefficient was divided into four levels for assessing sensitivity more clearly (Li et al., 2017), as shown in Table 1.

By multiplying the sensitivity coefficient of a single climatic variable by its relative change, we can get the change in ET_0 caused by the climatic variable, namely, the contribution rate of the climatic variable to ET_0 variation.

$$Conv_i = Sv_i \times RCv_i \tag{8}$$

$$RCv_i = \frac{n \times Trendv_i}{|Av_i|} \times 100\% \tag{9}$$

where $Conv_i$ is the contribution rate of v_i to ET_0 variation, %; SV_i represents the sensitivity coefficient of ET_0 to variable v_i; RCv_i is the relative change of v_i, %; n is the length of observations; $|Av_i|$ is the absolute value of the multi-year averaged v_i; and $Trendv_i$ is the estimated trend of the variable v_i. If the $Conv_i$ is positive (negative), the variation of the variable will increase (decrease) ET_0, denoting the variable had a positive (negative) contribution to ET_0 variation.

2.6. Spatial interpolation method

Inverse distance weighting (IDW) method gave the lower mean error than other common interpolation methods (spline, ordinary kriging) (Tang et al., 2013; Feng et al., 2017b), thus IDW from Arcgis 10.2 was applied to describe the spatial variability of ET_0 and other variables in the present research.

3. Results

3.1. Spatial distribution and changes in reference evapotranspiration (ET_0)

The temporal variation of averaged growing season ET_0 over the 99 meteorological stations in SC during the whole study period was plotted in Fig. 2. A change point for ET_0 series was discovered around the year of 1996 by the Cramer's test. Growing season ET_0 demonstrated a significant decreasing trend ($P < 0.05$) from 1961 to 1996 by 10.25 mm/decade, while turned into a significant increasing trend ($P < 0.05$) from 1997 to 2016 by 8.12 mm/decade.

Fig. 3 illustrates the trends in growing season ET_0 for the 99 meteorological stations in SC before and after the change point (1961–1996, 1997–2016) and the whole study period (1961–2016). Growing season ET_0 decreased at 90 out of 99 stations from 1961 to 1996, and ET_0 exhibited a statistically significant decreasing trend ($P < 0.05$) at 44 stations out of the 90 stations, which are mainly distributed in GB, SB and east of YGP. However, growing season ET_0 exhibited an increasing trend at 71 out of 99 stations from 1997 to 2016, and 27 stations in WSP and Southwest YGP showed a statistically significant increasing trend ($P < 0.05$). In general, growing season ET_0 exhibited a decreasing trend at 80 out of 99 stations from 1961 to 2016, and ET_0 showed a statistically significant decreasing trend ($P < 0.05$) at 34 stations out of the 80 stations, and the stations were mainly concentrated in GB, SB and east of YGP, while the stations whose ET_0 having significant increasing trends were mainly located on the western edge of the YGP.

The distribution of growing season ET_0 showed an obvious spatial gradient (Fig. 3). The ET_0 values increased from west to east whilst from north to south, and the mean growing season ET_0 of 99 meteorological stations was 665.6 mm, with the variation rang of 420.4 mm to 897.2 mm during the period 1961–2016. Regionally, the mean values between 500 and 750 mm occurred in the east of YGP and SB, while the southwest YGP and GB regions have the variation ranging between 750 and 900 mm with the highest values appeared in Beihai station near the ocean and a lowest mean growing season ET_0 in WSP.

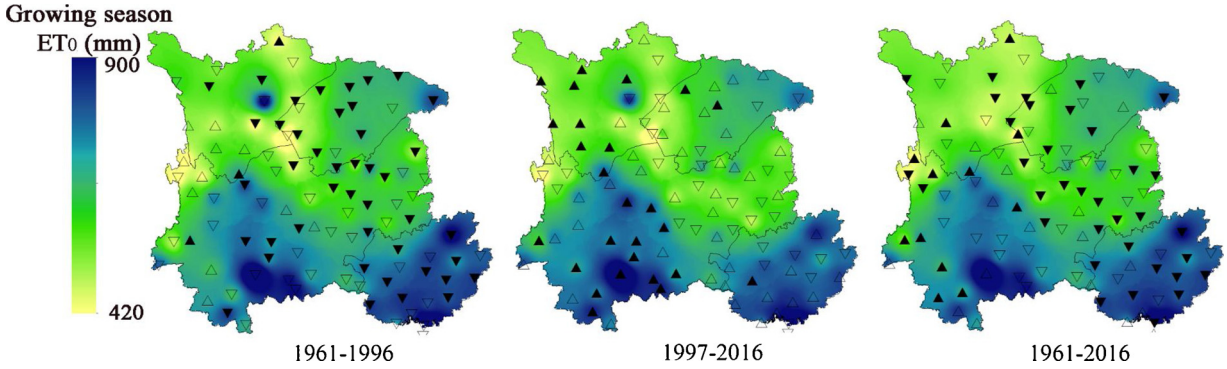

Fig. 3. Spatial distributions and trends of ET_0 in Southwest China (SC) during the period 1961–1996 (Left), 1997–2016 (Middle) and 1961–2016 (Right). ▲increased significant ($P < 0.05$), △increase, ▽decrease, ▼decreased significant ($P < 0.05$).

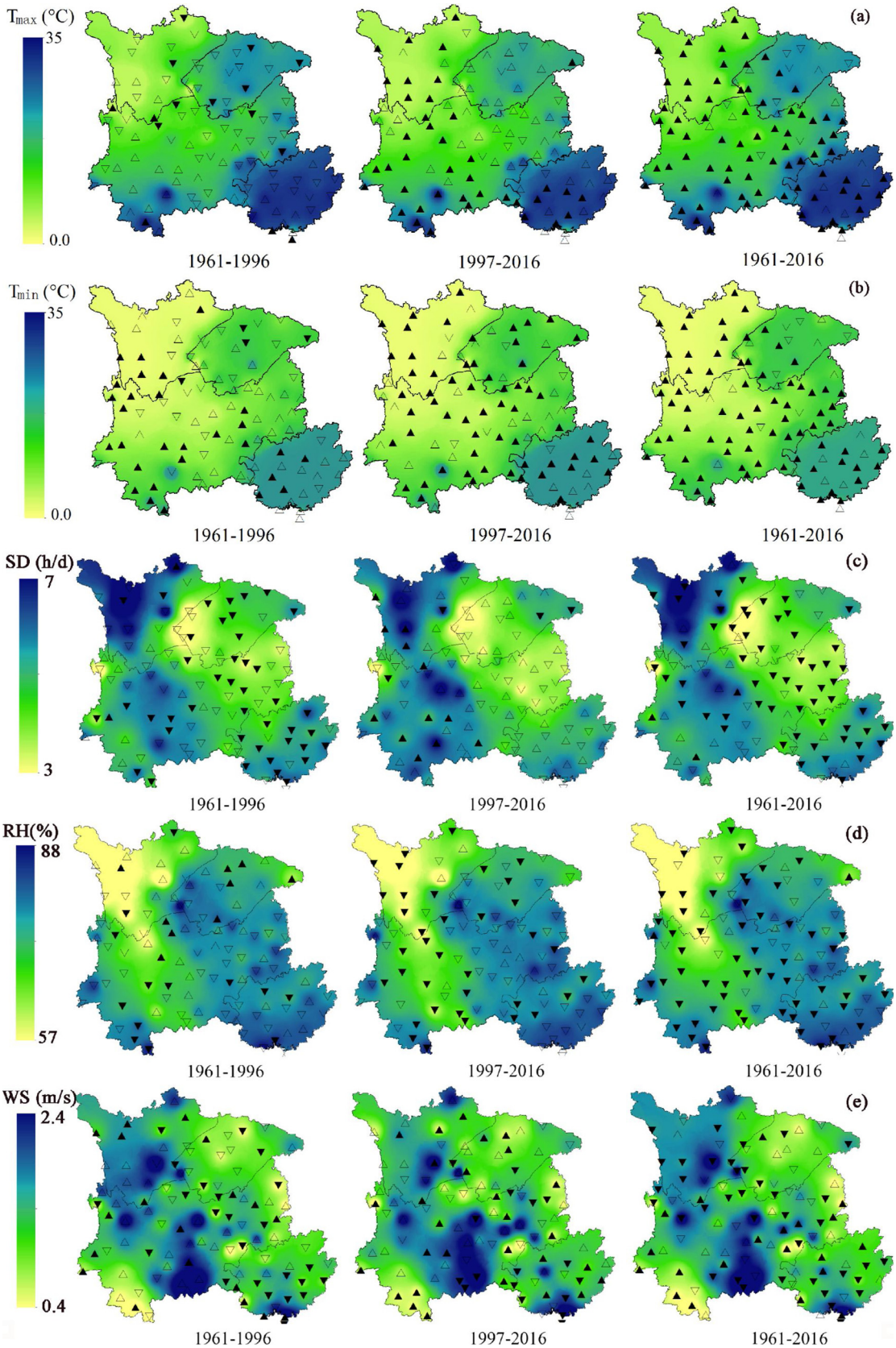

Fig. 4. Spatial distributions and trends of climatic variables (a) maximum air temperature (T_{max}), (b) minimum air temperature (T_{min}), (c) sunshine duration hours (SD), (d) relative humidity (RH), (e) wind speed at 2 m height (WS) in Southwest China (SC) during the period 1961–1996 (Left), 1997–2016 (Middle) and 1961–2016 (Right).▲increased significant ($P < 0.05$), △increase, ▽decrease, ▼decreased significant ($P < 0.05$).

Table 2
Average values and its Mann-kandall trend test and slope of growing season climatic variables (maximum air temperature (T_{max}), minimum air temperature (T_{min}), sunshine duration hours (SD), wind speed at 2 m height (WS), relative humidity (RH)) in Southwst China (SC) and its four sub-regions (WSP: Western-Sichuan Plateau; SB: Sichuan Basin; YGP: Yunnan-Guizhou Plateau; GB: Guangxi Basin).

		T_{max} (°C)			T_{min} (°C)			SD (h/day)			WS (m/s)			RH (%)		
Regions	Period	Average	Z	Slope	Average	Z	Slope	Average	Z	Slope	Average	Z	Slope	Average	Z	Slope
YGP	1961-1996	25.51	−0.34	−0.006	16.240	2.74**	0.012	4.97	−3.26**	−0.017	78.08	−1.43	−0.02	1.28	0.12	0.001
	1997-2016	25.96	2.11	0.039	16.880	2.43**	0.038	4.76	0.23	0.008	75.96	−1.91	−0.155	1.21	2.30*	0.009
	1961-2016	25.67	3.23**	0.012	16.470	6.14**	0.021	4.90	−3.63**	−0.010	77.32	−4.53**	−0.066	1.25	−1.86	−0.001
WSP	1961-1996	18.78	−0.97	−0.004	6.650	3.28**	0.018	5.63	−1.10	−0.004	70.11	0	−0.004	1.57	1.05	0.005
	1997-2016	19.51	2.24*	0.054	7.590	1.98*	0.045	5.33	1.33	0.019	68.17	−1.91	−0.173	1.38	3.08**	0.013
	1961-2016	19.05	3.39**	0.019	6.990	6.62**	0.030	5.53	−2.76**	−0.008	69.42	−3.30**	−0.057	1.50	−2.11*	−0.003
GB	1961-1996	30.35	0.29	−0.002	22.820	1.76	0.007	5.43	−3.99**	−0.028	81.01	−0.91	−0.007	1.37	−3.31**	−0.004
	1997-2016	30.77	1.72	0.033	23.350	2.63**	0.033	5.12	−0.16	−0.001	78.78	−1.33	−0.134	1.35	0.10	0.000
	1961-2016	30.50	1.82	0.011	23.010	3.30**	0.016	5.32	−3.81**	−0.015	80.22	−2.44**	−0.063	1.36	−2.63**	−0.001
SB	1961-1996	27.43	−1.46	−0.016	19.390	−0.80	−0.004	4.54	−2.10*	−0.024	78.12	1.29	0.036	1.05	−3.71**	−0.004
	1997-2016	28.36	1.46	0.033	19.970	2.50**	0.032	4.20	−0.23	−0.004	75.54	−1.69	−0.181	1.01	2.43**	0.008
	1961-2016	27.83	2.60	0.019	19.650	3.02**	0.015	4.43	−2.66**	−0.015	77.38	−1.86	−0.007	1.03	−1.37	−0.001
SC	1961-1996	26.00	−0.39	−0.006	16.940	2.01*	0.009	5.08	−3.05**	−0.019	77.7	−0.52	−0.007	1.30	−1.28	0.000
	1997-2016	26.56	1.94	0.039	17.580	2.43**	0.037	4.82	0.21	0.006	75.5	−1.75	−0.157	1.23	1.96	0.008
	1961-2016	26.21	2.69*	0.014	17.180	4.88**	0.020	4.99	−3.48**	−0.011	76.95	−3.21**	−0.066	1.27	−2.53**	−0.001

* Indicates significance levels of 0.05.
** Indicates significance levels of 0.01.

3.2. Spatially distribution and changes in climatic variables

Spatially averaged T_{max}, T_{min} showed a general increase trend, while RH, SD, WS showed a significant downward trend in the study area over the past 56 years (Fig. 4). Trend analysis indicated that T_{min}, T_{max} in SC have increased significantly ($P < 0.01$) by 0.14 °C, 0.2 °C / decade, respectively. In contrast, SD, WS and RH decreased significantly by 0.11 h, 0.01 m/s, 0.6% /decade from 1961 to 2016 respectively (Table 2). T_{max} and T_{min} have also obviously increased with multiple trends. The growth rates of T_{max} (0.2 °C / decade) and T_{min} (0.3 °C / decade) were largest in the WSP, while the rates of T_{max} (0.11 °C / decade) in GB and T_{min} (0.15 °C / decade) in SB were smallest. SD, WS and RH have been decreasing across different regions. SD had a significant decrease trend ($P < 0.01$) in all regions, with the highest rate (−0.15 h/ decade) in SB and GB and the lowest (−0.08 h/ decade) in WSP. WS in YGP and SB, and RH in SB showed an insignificantly decreased trend ($P > 0.05$) by -0.01 m/s /decade and −0.76%/decade, respectively, while decreased significantly in the other regions.

The variations of each climatic variable before and after the change point was shown in Fig. 4 and Table 2. T_{min} increased by 0.09 °C/decade, while T_{max} decreased by 0.06 °C/decade from 1961 to 1996, respectively. However, T_{min} increased significantly ($P < 0.05$) by 0.37.°C /decade while T_{max} increased by 0.39 °C /decade from 1997 to 2016 in SC. The similar changes of T_{max} and T_{min} were also detected in four sub-regions. SD had a significantly decreased ($P < 0.05$) trend in most of the stations, with the rate of −0.19 h/decade from1961 to 1996 in SC, while an insignificant increasing trend after 1996 mainly occurred in WSP and YGP. RH showed a downward trend in SC, then decreased significantly after 1996 with a rate of −1.57%/decade (Table 2). WS decreased significantly ($P < 0.001$) with the rate of −0.04 m/s/decade in SB and GB from 1961 to 1996, while increased by 0.01 m/s/decade and 0.05 m/s /decade in YGP and WSP, however, WS increased significantly ($P < 0.05$) in SC except for GB after 1996.

3.3. The variations of sensitivity coefficients characteristics during the growing season

In order to quantify the sensitivity of ET_0 to climate variables, the average sensitivity coefficients for T_{min} (S_{Tmin}), T_{max} (S_{Tmax}), RH (S_{RH}), SD (S_{SD}) and WS (S_{WS}) in SC and its four sub-regions were calculated and the results were shown in Fig. 5 and Table 3. The notation of the sensitivity coefficients shows that ET_0 is positively correlated to the vary of T_{max}, T_{min}, SD and WS, while negatively correlated to the vary of RH. In addition, it can be seen from Fig. 5 and Table 3 that ET_0 was most sensitive to RH in SC from 1961 to 2016, with the average sensitivity coefficient value −0.496, followed by SD (0.284), T_{max}(0.208), T_{min}(0.080) and WS(0.052). However, the most sensitive climatic variable was RH, followed by SD, T_{max}, WS, and T_{min} in WSP and SB, while by SD, T_{max}, T_{min} and WS in GB from 1961 to 2016. S_{Tmin} ranged from 0.008 to 0.17 throughout the study area, with medium levels in GB and SB, but negligible levels in YGP and WSP. S_{Tmin} had an obvious increasing trend during the period 1961–2016 at most stations with high altitudes, while it increased weakly or decreased at most stations with low altitudes of SC. S_{Tmax} varied from 0.06 to 0.41 with a medium level in most regions except for WSP. S_{Tmax} had an increasing trend before 1996 and a more obvious increasing trend from 1997 to 2016. S_{RH} in most regions had a high level and the lager values were distributed mainly in GB and east of YGB. Strong negative sensitivity shows an increase in RH would greatly reduce ET_0. The changed trend in S_{RH} had a lager difference in spatial distribution, S_{RH} displayed an increasing trend in GB and decreasing trends in other regions from 1961 to 1996, however, S_{RH} was decreasing after 1997 throughout the study area. S_{SD} ranged from 0.17 to 0.39 and had a medium level in SC except for SB and east of YGP. S_{SD} in SC showed an obvious decreasing trend in most regions during the period 1961–1996, continued to decrease until 2016. S_{WS} ranged from 0.02 to 0.17 and had a medium level in WSP while the levels in other regions could be negligible. S_{WS} showed significantly increasing trends from 1961 to 2016, indicating that ET_0 was more sensitive to the change of WS.

The average monthly sensitivity coefficient on the T_{max}, T_{min}, SD, WS and RH during the growing season in SC and its four sub-regions (WSP, SB YGP and GB) were shown in Fig. 6. The sensitivity coefficients for climate variables are unstable during the growing season. S_{Tmin}, S_{SD} had a peak and reached maximum in July and August, demonstrating that ET_0 was most sensitive to the changes in T_{min} and SD in July and August. In the contrast, S_{WS} and S_{RH} were the largest at the beginning of the growing season, reached its minimum in July and August and rebounded at the end the growing season, indicating that ET_0 was least sensitive to the changes in WS and RH in July and August. The trends of S_{Tmax} in SC and its four sub-regions existed a large difference, Fig. 6 showed that ET_0 was sensitive to T_{max} at the early growing season in SC and its four sub-regions with the coefficient value around 0.23, however, S_{Tmax} decreased in most regions except GB in April and May. The characteristics of S_{Tmax} in YGP and WSP were steady with the sensitivity

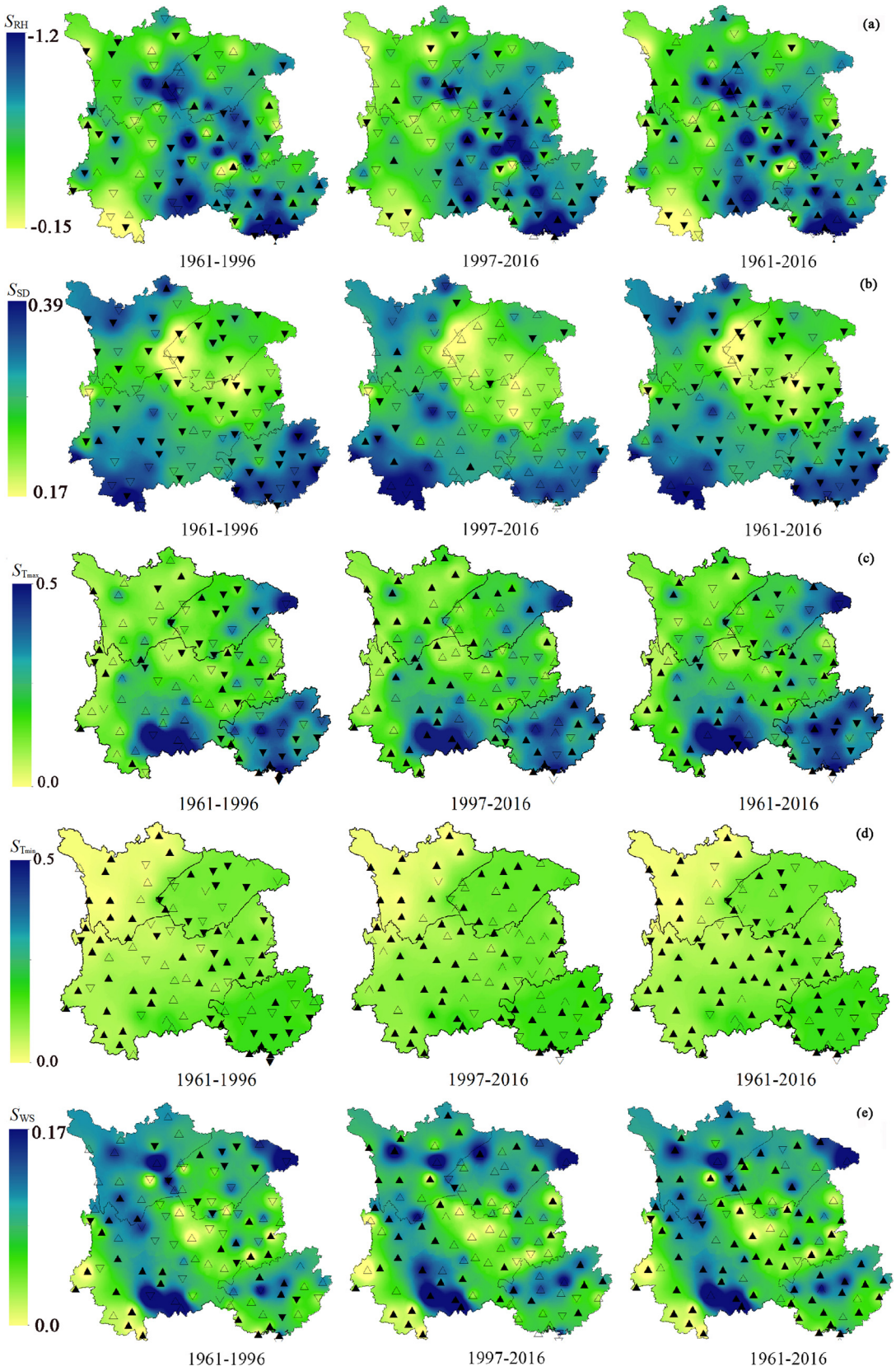

Fig. 5. Spatial distributions and trends of the sensitivity coefficients for (a) relative humidity (S_{RH}), (b) sunshine duration hours (S_{SD}), (c) maximum air temperature (S_{Tmax}), (d) minimum air temperature (S_{Tmin}), (e) wind speed at 2 m height (S_{WS}) in Southwest China (SC) during the period 1961–1996 (Left), 1997–2016 (Middle) and 1961–2016 (Right). ▲increased significant ($P < 0.05$), △increase, ▽decrease, ▼decreased significant ($P < 0.05$).

Table 3
The sensitivity coefficients for relative humidity (S_{RH}), sunshine duration hours (S_{SD}), maximum air temperature (S_{Tmax}), minimum air temperature (S_{Tmin}), and wind speed at 2 m height (S_{WS}) in Southwest China (SC) and its four sub-regions (WSP: Western-Sichuan Plateau; SB: Sichuan Basin; YGP: Yunnan-Guizhou Plateau; GB: Guangxi Basin).

Regions	Period	S_{RH}	S_{SD}	S_{Tmax}	S_{Tmin}	S_{WS}
YGP	1961–1996	−0.4750	0.2930	0.1980	0.0690	0.0420
	1997–2016	−0.4520	0.2730	0.2030	0.0750	0.0560
	1961–2015	−0.4600	0.2820	0.1970	0.0700	0.0470
WSP	1961–1996	−0.4650	0.2890	0.1810	0.0270	0.0410
	1997–2016	−0.4170	0.2770	0.1840	0.0320	0.0550
	1961–2016	−0.4470	0.2850	0.1820	0.0290	0.0460
GB	1961–1996	−0.6170	0.3220	0.2410	0.1200	0.0500
	1997-2016	−0.6160	0.3030	0.2610	0.1310	0.0700
	1961–2016	−0.6170	0.3150	0.2480	0.1240	0.0570
SB	1961–1996	−0.4910	0.2570	0.2030	0.0880	0.0580
	1997–2016	−0.4780	0.2370	0.2260	0.0960	0.0780
	1961–2016	−0.4870	0.2500	0.2120	0.0910	0.0650
SC	1961–1996	−0.5060	0.2920	0.2060	0.0780	0.0460
	1997–2016	−0.4860	0.2740	0.2170	0.0850	0.0630
	1961–2016	−0.4960	0.2840	0.2080	0.0800	0.0520

coefficient around 0.17, while a larger increase from July to September occurred in SB. The sensitivity of ET_0 to the same climate variable varied in four sub-regions, probably due to different climate as well as substrate layer characteristics in each region.

3.4. Contribution from climatic variables during the growing season

In order to identify the main climatic variables to ET_0 variation in SC and its four sub-regions, the relative contribution method was adopted to quantify the contribution of climatic variables to ET_0 change, and the results were shown in Table 4. SD was an important climatic variable effecting growing season ET_0 trends, causing reduced ET_0 by 3.96%, thereby becoming the largest contributor to the decreasing growing season ET_0 from 1961 to 1996. In addition, decreasing WS and T_{max} also played negative effects on growing season ET_0 in SC, with the contribution rate −0.14% and −0.15% from 1961 to 1996, respectively. Decreasing RH was the mainly contributor to increased ET_0 after 1996, which caused ET_0 to change by 1.99% from 1997 to 2016. In addition, increasing T_{max}, T_{min}, and WS also played an important effect on increased ET_0, and the contribution rate was 0.63%, 0.34%, and 0.74%, respectively in SC, from 1997 to 2016. The same patterns were also found in its sub-regions. However, the same climate variable may have different contribution rates to the change of ET_0 in four sub-regions because of the different sensitivities and change in climate variable in terms of spatial distribution.

The average monthly contribution rates for climatic variables during the growing season in SC and its four sub-regions (WSP, SB YGP and GB) are shown in Fig. 7 and Table 4. Results showed that the increase of T_{max}, T_{min}, and the decrease of RH had positive contributions to ET_0 during the growing season, while the decrease of WS and SD had negative contributions to ET_0. The contribution rate of T_{max} was higher in WSP but the S_{Tmax} in WSP was lower, indicating that T_{max} had a lager increase in WSP, and had a peak in June indicating that the T_{max} in June increased greatly. The similar variation characteristics were also found in the contribution rates of T_{min}. The contribution rates of T_{min} and WS was higher in April while the lower value appeared in August, and the opposite characteristics appeared in the contribution rate of SD, revealed that the variation of T_{min} and WS was small while SD varies greatly at the end of the growing season. The contribution rate of RH reached its minimum in June in most regions and rebounded at the end the growing season. The lowest value was close to 0 in WSP at the beginning of the growing season indicating that RH in WSP had small variation in April. Results in Fig. 7 clearly showed that RH was the main climatic variable causing ET_0 variation at the beginning of the growing season in SC, followed by SD, WS, T_{max}, T_{min}. At the middle and late stages of growing season the biggest contributor to ET_0 was SD with the highest value -6.95% in July. As shown in Table 3 that ET_0 was most sensitive to RH, but a significant reduction in SD caused a great decline of ET_0. Thus, the contribution rate of SD was most important to the changes of ET_0.

4. Discussion

4.1. Patterns of reference evapotranspiration and climatic variables

Understanding the spatial and temporal evolutions of ET_0 in growing season is the initial step in calculating regional crop evapotranspiration and irrigation water planning. Probing the effects of climatic variables on ET_0 variation will assist in predicting the variation of ET_0 in the context of climate change (Tong et al., 2007; Feng et al., 2017c). However, because of the diversity of the regional geography and the climatic conditions, it was necessary to carry out a regional research to provide a reference framework for providing basic scientific evidence for agricultural activities, water resources planning and management.

A change point for ET_0 series was discovered in 1996 by the Cramer's test in this study. Growing season ET_0 had demonstrated a significant decreased trend during 1961–1996, while turned into a significantly increased trend from 1997 to 2016. Li et al. (2014b) also indicated that annual ET_0 had a decreased trend during 1960–2000 and an increased trend during 2000–2009 in Southwestern China (SC), which was well coincident with the results obtained in this research. Liu et al. (2018) detected a turning point of annual PET series in SC, and annual PET had a downward trend at -10.04 mm/dacade during 1961–2000, but increased at 50.65 mm/decade thereafter. Such abrupt changes of ET_0 have been widely reported in many regions of the world. Li et al. (2016) found annual ET_0 decreased significantly ($P < 0.05$) in the Loess Plateau by 12.22 mm/decade from 1960 to 1990, while it increased significantly ($P < 0.001$) by 11.5 mm/decade from 1991 to 2013, Papaioannou et al. (2011) discovered that the trend of annual ET_0 in Greece had a declined trend before the early 1980s, conversely, it has begun to increase until 2001. Zhang et al. (2007) found the annual ET_0 decreased at 10.5 mm/dacede in Tibetan Plateau from 1966 to 2003, however, the increasing ET_0 was not detected because of the shorter research period (only to 2003). In addition, Liu and Zhang (2013) detected an increased ET_0 after 1993 in Northwest China. Liu et al. (2011) investigated the pan evaporation in China, and found it decreased from 1960 to 1991 while increased after 1992. The variation of ET_0 in this paper are generally consistent with the previous reports. However, the change point and variation range of ET_0 series may exist difference due to the different study areas and study period.

The decreasing SD was found at most stations of SC, which is consistent with many previous researches in China (Zhang et al., 2007; Qian et al., 2007; Li et al., 2015; Wang et al., 2017). However, the reasons for SD change remains subject to debate. Cong et al. (2009) thought that the increase in cloud cover may be the main reason causing SD reduction. However, the assumption that the increase in cloud cover causing SD reduction at SC seems to be unreasonable as declining precipitation had been widely reported in many regions of the world (Ruelland et al., 2008; Feng et al., 2017b). Recent studies showed that aggregated aerosols from anthropogenic emissions of pollutants were main dimming factor (Qian et al., 2007; Zhao et al., 2014), Streets et al. (2008) and Feng et al. (2017b) found that there was significant decline in SD in Southwest China, the same conclusion was also obtained in this research. In addition, as can be seen, stations with significant decrease in SD are mainly distributed at low altitudes of the study area, where the population density is higher and human activity is concentrated. Industry in these areas is well developed, pollution is more serious in such areas than in low population density areas such as YGP. Hence the decrease of SD is more visible at the low altitudes than

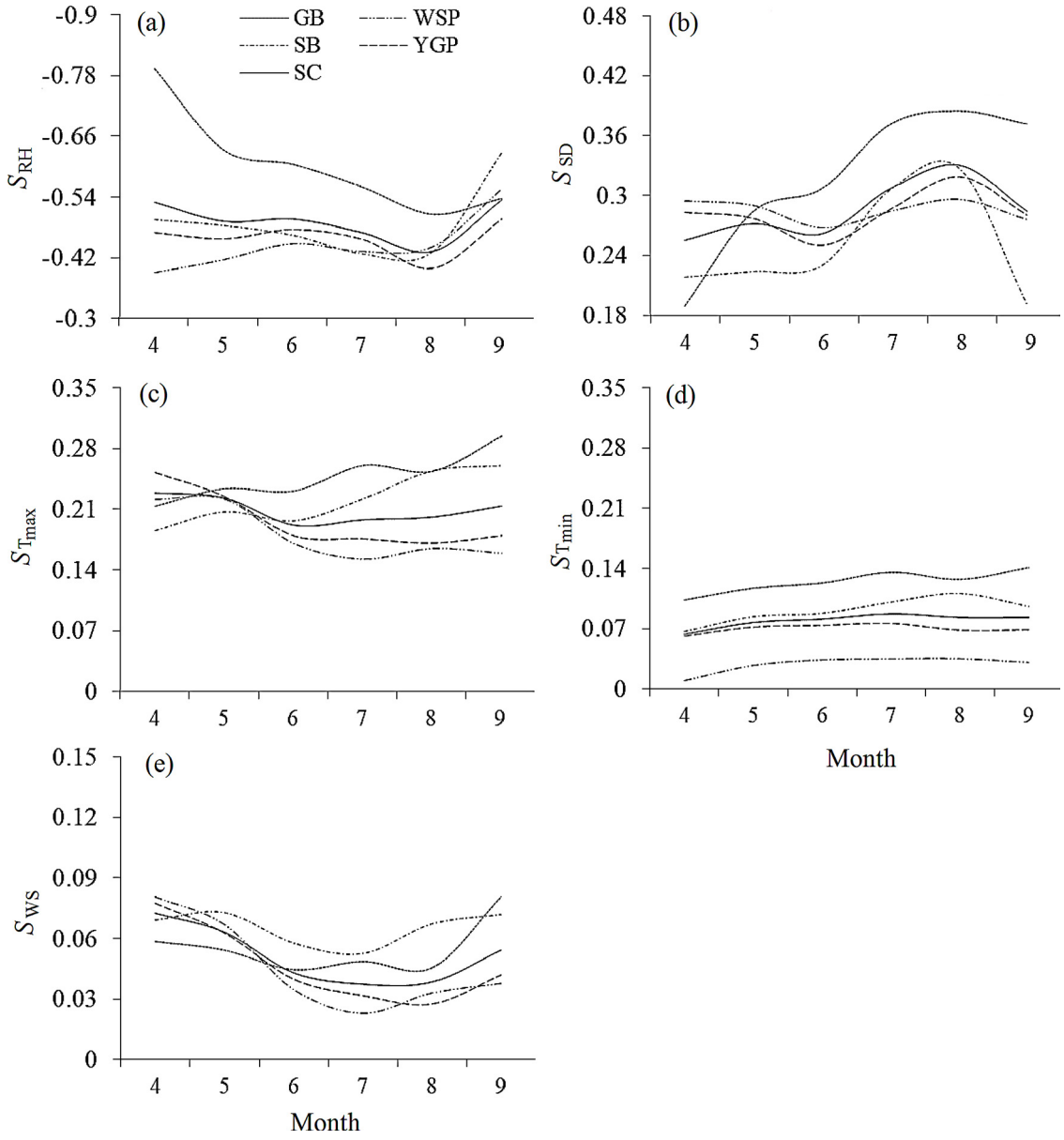

Fig. 6. The sensitivity coefficients for (a) relative humidity (S_{RH}), (b) sunshine duration hours (S_{SD}), (c) maximum air temperature (S_{Tmax}), (d) minimum air temperature (S_{Tmin}), (e) wind speed at 2 m height (S_{WS}) in Southwest China (SC) and its four sub-regions (WSP: Western-Sichuan Plateau; SB: Sichuan Basin; YGP: Yunnan-Guizhou Plateau; GB: Guangxi Basin) during the growing season.

the high altitudes, deducing that the increase in aerosols resulting from human activities may be an important reason for the decrease in solar radiation (Grimenes and Thue-Hansen, 2006; Qian et al., 2007). Zhao et al. (2014) investigated climatic variables in two elevation groups (plains and mountains) in Hai River Basin, and found the decreasing trend of solar radiation was more significant in the densely populated areas (plains) than in the sparsely populated ones (mountains). Aerosol index increased more and more significantly from the low population density areas in northern China such as Yanshan and Taihang mountainous areas to the high population density areas, the spatial distribution of the aerosol index increase is consistent with the solar radiation decrease. Wang et al. (2017) indicated that the high-rise buildings in urban area can be obstacles to the flow of wind, making the atmospheric aerosol difficult to diffuse, thereby aggravating the decrease of SD. It can be concluded that human activities do have an important impact on the changes of solar radiation or SD, from the above studies. WS, which has a larger fluctuation in SC and its four sub-regions is also the main climatic factor affecting the change of ET_0. The variations of WS in SC and its four sub-regions from 1961 to 2016 were shown in Fig. 8.

WS showed a statically significant decrease in 1960s, while increased rapidly in late 1960s, then decreased significantly until 2000, and gradually increased in recent years. The same change trend of WS was also founded by Li et al. (2014b) and Fu et al. (2010), and the decline in WS was not significant throughout the whole study period. Generally, a weakened atmospheric circulation is thought to be the reason for WS decline (Zhang et al., 2009). The temperature difference between the polar and tropical areas associated with global warming has been declining, weakening the strength of atmospheric circulation. Weak atmospheric circulation has been proved in East Asian and South Asian (Xu et al., 2006; McVicar et al., 2012). Additionally, recent studies showed that the increasing surface roughness result from human activities, such as plantation and urbanization nearby the weather stations may also play an important role in the decreasing WS (Shi et al., 2017). However, the WS in some meteorological stations have exhibited significant increasing trends since 2000, while the vegetation

Table 4
Contributions to ET_0 from the relative change of the climate variables sunshine duration hours (SD), maximum air temperature (T_{max}), minimum air temperature (T_{min}), relative humidity (RH), wind speed at 2 m height (WS) in Southwest China (SC) and its four sub-regions (%). (WSP: Western-Sichuan Plateau; SB: Sichuan Basin; YGP: Yunnan-Guizhou Plateau; GB: Guangxi Basin).

Regions	period	SD	RH	WS	T_{max}	T_{min}
YGP	1961–1996	−3.5304	0.4301	0.1298	−0.1501	0.1766
	1997–2016	0.9382	1.8095	0.8152	0.5944	0.3275
	1961–2016	−3.0345	2.1438	−0.2333	0.4889	0.4899
WSP	1961–1996	−1.8028	0.1007	0.5037	−0.1461	0.2734
	1997–2016	0.9000	2.1142	1.0373	1.0187	0.3750
	1961–2016	−3.2010	2.0497	−0.4414	1.0321	0.6963
GB	1961–1996	−6.0441	0.1887	−0.5711	−0.0696	0.1233
	1997-2016	−0.1365	2.0961	0.0087	0.5614	0.3749
	1961–2016	−5.0487	2.7079	−0.3372	0.5137	0.4919
SB	1961–1996	−4.2481	−1.4166	−0.9037	−0.2262	0.0114
	1997–2016	−0.4051	2.2941	1.2160	0.5331	0.3093
	1961–2016	−4.5090	1.9396	−0.6463	0.9362	0.4099
SC	1961–1996	−3.9577	0.0309	−0.1417	−0.1455	0.1501
	1997–2016	0.4857	1.9881	0.7417	0.6304	0.3403
	1961–2016	−3.7207	2.2155	−0.3498	0.6365	0.5028

cover continued to increase (Liu and Zhang, 2013; Liu et al., 2008). Changes in surface roughness may not fully explain the changes in WS. Therefore, the driving factors of changes in WS need to be fully understood in SC. Air temperature showed significant increasing trends at most stations in the study area, consistent with global warming from previous researches (Li et al., 2014a; Najafi et al., 2015; Feng et al., 2017b). However, diurnal temperature range had the downward trend because the increase in T_{min} was more obviously than the T_{max}, which may be due to that aerosols and greenhouse gases absorb solar radiation during daytime and release energy in the form of long-wave radiation into the atmosphere at night (Liu et al., 2010). Increasing aerosols and anthropogenic greenhouse gases emissions (Najafi et al., 2015), and urbanization (Ji and Zhou, 2011) are widely considered to be the primary reasons for temperature increase. However, the increasing trends of T_{max} and T_{min} (with the rate of 0.14 and 0.20 °C/decade, respectively) in this study were generally lower than those reported in other parts of the world (IPCC, 2007), this may be related to higher vegetation and forest coverage in SC. The decline of RH mainly resulting from the decreasing trend in precipitation in Southwest China (Yan et al., 2013; Feng et al., 2014), will have a vital impact on the variation of evapotranspiration. The decrease of relative humidity is more significant in most sites of the high-altitude areas, which was also discovered by Zhao et al. (2014). The decline of RH will reduce atmospheric vapor pressure and accelerate the release of water vapor from plant stoma.

The spatial distribution characteristics of climatic variables were similar to previous studies of SC and parts of this region (Gong et al., 2006; Li et al., 2014b; Liu et al., 2017; Feng et al., 2017b), while temporal trend may exist difference because of the different study period. It is interesting to note that the spatial distribution of climatic variables shows the border line at appa. at 105 °E (Yin et al., 2010; Feng et al., 2017b), which appears to point to the influence of different monsoon, especially during the growing season, the water stream originating from South China Sea transported by Southeast monsoon and from Bay of Bengal transported by Southwest monsoon, forming a wet center at the east of 105 °E of study area because of the obstruction of the mountains (Fan and Thomas, 2013; Liu et al., 2018), besides, the gather water vapor in this region can markedly weaken solar radiation, therefore, SD is far lower than that of the west of 105 °E of study area.

4.2. Sensitivity and contribution rate of ET_0 to the variation of climatic variables

The sensitivity coefficients of climatic variables calculated in this paper are close to the previous studies in China or other regions (Zuo et al., 2012; Zhang et al., 2013; Gao et al., 2016; Li et al., 2017). Researches had found RH was the most sensitive variable in the Wei River basin, and also the most sensitive factor in the Yellow River basin (Wang et al., 2007; Zuo et al., 2012) and Hai River basin (Zhao et al., 2014), Gong et al (2006) found that relative humidity was the most sensitive variable to ET_0 change in Yangtze River basin, followed by shortwave radiation, air temperature and wind speed was the least sensitive variable, Liu et al (2018) indicated that the spatial distribution of annual ET_0 is mainly affected by air temperature, sunshine hours and relativity humidity over Southwest China, while SD was the most sensitive climatic variable in Poyang Lake catchment (Ye et al., 2014), and WS had the highest sensitivity in Northwest China (Li et al., 2014a). The differences existed may be due to differences in the study areas and calculation methods. The contribution rate of climate variable was determined not only by the sensitivity of ET_0 to climatic variable, but also by the magnitude of the climatic variables trends. Although RH was the most sensitive climatic variable for ET_0, it contributed little to ET_0 change due to its much smaller change magnitude during the period 1961–1996 in the present study. The sensitivity coefficient of SD was not the highest, but SD contributed the most to ET_0 change among the variables due to its rather large variation during the period 1961–1996. The magnitude of the RH trend was large from 1997 to 2016, thus causing the contribution rate of RH to ET_0 was much greater among the variables during the period 1997–2016. Zhao et al. (2014) also found that the sensitivity order of climatic variables to ET_0 from strong to weak was: relativity humidity, temperature, shortwave radiation and wind speed in Hai River Basin, respectively, however, and the decreasing ET_0 was caused mainly by the decreasing wind speed and shortwave radiation. Liu and Zhang (2013) found the decreases in vapor pressure deficit, wind speed, and solar radiation had more effects on the changes of ET_0 than increasing air temperature before 1993 in Northwest China, and Zhang et al. (2015) investigate the temporal trends of ET_0 in the Yellow River Basin from 1961 to 2012, the results showed that the change of sunshine hours was the major factors influencing the variability of ET_0, followed by wind speed, Li et al. (2014b) found that the decreased relative humidity would cause a corresponding decline of saturated vapor pressure, which must lead to the rise of ET_0 during the period of 1991–2009 in Southwestern China, which was well coincident with the results obtained in this research. While Li et al. (2016) found annual ET_0 decreased significantly ($P < 0.05$) in the Loess Plateau from 1960 to 1990, and wind speed was mostly responsible for the variability in the ET_0 trend from 1960 to 1990, followed by solar radiation and vapor pressure, while it increased significantly ($P < 0.001$) from 1991 to 2013 because of the rapidly increasing air temperature. The variation of ET_0 in this paper are generally consistent with the previous reports (Li et al., 2014b; Li et al., 2016). However, the dominant fctors on ET_0 variation may exist difference due to the different study areas and methods adopted.

Increasing temperature (including T_{min}, T_{max}) should have led to the increase of ET_0 before 1996, but ET_0 had a decreased trend in this period, so “Evaporation paradox” also existed in SC. Significant decrease in SD and WS offsets the impact of increasing temperature and decreasing RH, dominating the change in ET_0 in SC (Yin et al., 2010; Zhang et al., 2013; Feng et al., 2017b), finally resulted in “evaporation paradox” in SC before 1996.

The uncertainties in the estimation of the contribution of climate variable to ET_0 variation existed in present research, as the variables change rates and sensitivity coefficients were not the same but fluctuated. Therefore, the average values were used to estimate the contribution to ET_0 variation might be less accurate (Liu and Zhang, 2013; Fan et al., 2016).

4.3. Implications of ET_0 changes on agricultural water management

In order to analyze the crop water demand variations for crops in

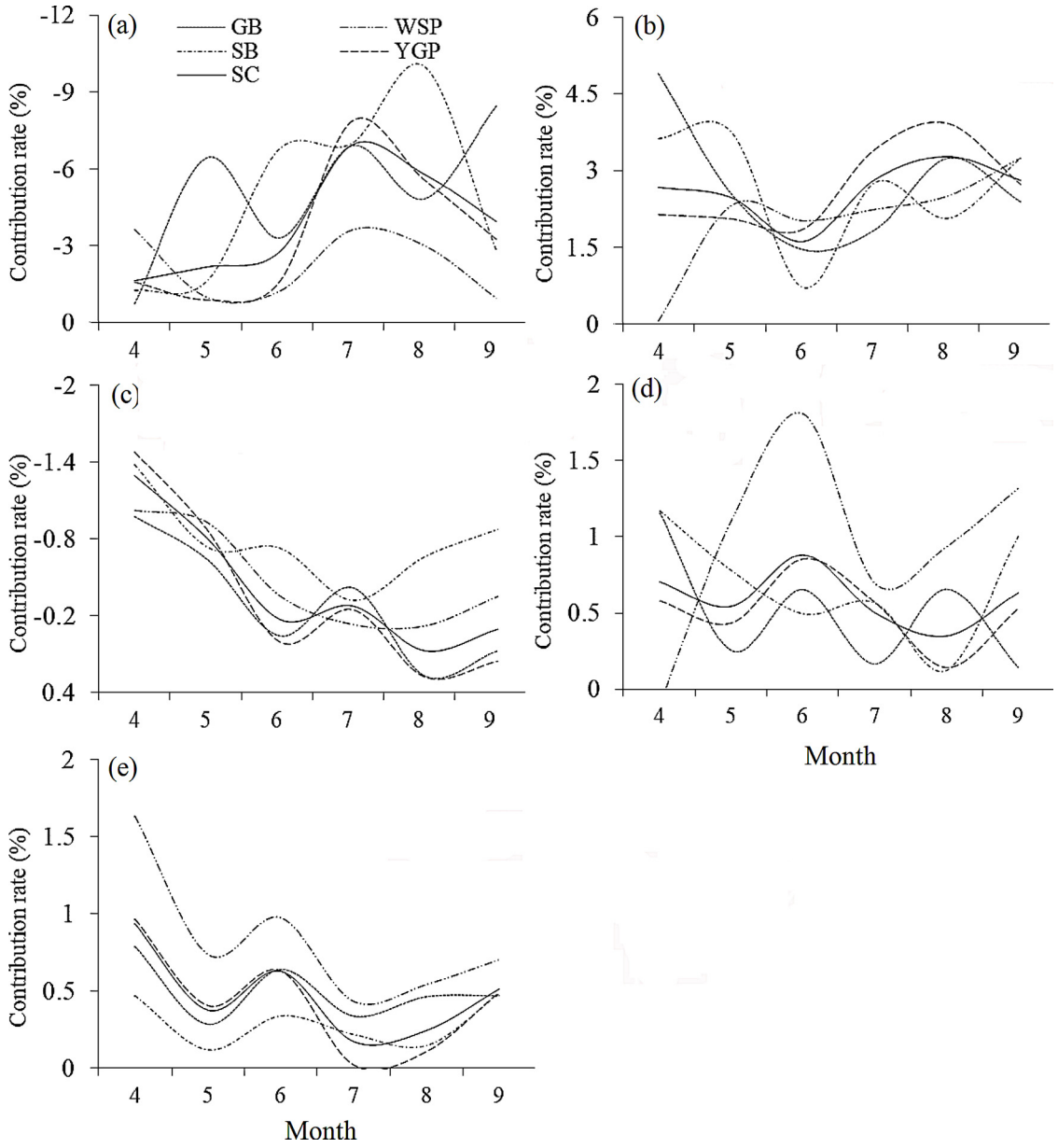

Fig. 7. Contributions of the climatic variables (a) sunshine duration hours (SD), (b) relative humidity (RH), (c) wind speed at 2 m height (WS), (d) maximum air temperature (T_{max}), (e) minimum air temperature (T_{min}) to ET_0 variations in Southwest China (SC) and its four sub-regions (WSP: Western-Sichuan Plateau; SB: Sichuan Basin; YGP: Yunnan-Guizhou Plateau; GB: Guangxi Basin) during the growing season months (1961–2016).

growing season, and provide general profiles of crop water demand in each subregion of SC, actual crop water demand during the growing season is estimated by multiplying daily ET_0 by a modified crop coefficient K_c (Allan et al., 1998; Kang et al., 2003; Thomas, 2008). Crop coefficients during different growth stage of different crops are modified according to Allan et al. (1998) and listed in Table 5.

The application of multiple cropping systems is benefit for characterizing the evolution features of crop water demand, however, multiple cropping systems are adopted in this region, we mainly selected two representative cropping systems in each subregion except for WSP for analyzing as a simplification. Seeing that the same subregion has similar crop planting types and intercropping has not been accounted for, the results are shown in Table 6.

Both early rice-late rice and corn-late rice cropping systems in GB are two large water consumers, while highland barley in WSP consumed less water with the multi-year averaged value of 479 mm, which is due to low ET_0 values and single cropping system. It is interesting to note that actual crop water demand during the growing season were detected to have increased trends in each regions of SC after 1996, especially for WSP and YGP, appeared to have experienced a more significant increase ($P < 0.05$) from 1997 to 2016, though crop water demand generally appears as decreasing trends from 1961 to 2016. Meanwhile, studies have showed that the precipitation in SC had a declining trend in recent years (Xu et al., 2006; McVicar et al., 2012) because of the impact of West Pacific subtropical high as well as South Asia high (Yan et al., 2013; Liu et al., 2017), indicating crops is more likely to be threatened by drought, especially for rainfed agriculture areas in SC. A warm and dry environment may slow the restoration of vegetation, causing ecological problems such as grassland degradation and soil erosion. This will have a negative impact on the economic and ecological environment of the WSP area dominated by animal husbandry. The YGP, with a thin soil layer weathered by rocks, leading to lower soil moisture storage and thus aggravated water shortage (Jiang et al., 2018). However, it is difficult to construct a large water

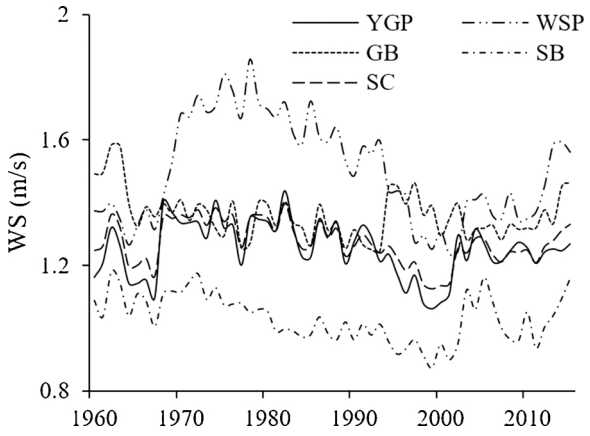

Fig. 8. Wind speed (WS) variations in Southwest China (SC) and its four sub-regions (WSP: Western-Sichuan Plateau; SB: Sichuan Basin; YGP: Yunnan-Guizhou Plateau; GB: Guangxi Basin) from 1961 to 2016.

Table 5
Crop coefficients during growing season and cropping systems of four sub-regions (WSP: Western-Sichuan Plateau; SB: Sichuan Basin; YGP: Yunnan-Guizhou Plateau; GB: Guangxi Basin) in Southwest China (SC).

Regions	Cropping systems	Crop coefficients					
		April	May	June	July	Augest	September
YGP	Rape-Rice	0.85	1.28	1.26	1.32	1.36	1.27
	Early rice-Late rice	1.22	1.25	1.34	1.20	1.26	1.33
WSP	Highland barley	0.44	0.85	1.24	1.26	0.72	
GB	Early rice-Late rice	1.18	1.20	1.32	1.18	1.25	1.28
	Corn-Late rice	1.04	1.25	1.30	1.05	1.25	1.28
SB	Rape-Rice	0.85	1.27	1.24	1.29	1.33	1.24
	Wheat-Rice	0.75	1.08	1.25	1.29	1.33	1.24

conservancy project because of the poor geology and limited available technology. Therefore, more drought-resistant species and irrigation facilities are required to maintain the crop production in YGP. Though the increased trend of crop water demand in SB is not significant as YGP and WSP, the increasing crop water demand will significantly affect regional agricultural water management. SB is not only one of the most developed agriculture regions, but also a densely populated area in China, the consumption of industrial water and domestic water has been increasing rapidly with the rapid growth of the economy and urban population in recent decades (Qian et al., 2007), which will occupy more available water resources, the main crops may suffer serious water shortage threat in SB because of the extraordinary industrialization and urbanization in this area. The development of water-saving irrigation to improve the utilization efficiency of water resources is an important way to deal with the agricultural water shortage (Mushtaq et al., 2006), the measures of water-saving irrigation in SB need to be considered through the aspects of engineering (drip irrigation, micro-irrigation, etc.), agronomy (regulated deficit irrigation, water-saving varieties, etc.), management (water price, government police, etc.) and so on, under the trend of agricultural water shortages (Ørum et al., 2010; Nyakudya and Stroosnijder, 2014; Li et al., 2016; Pérez-Sarmiento et al., 2016). Therefore, the administration of SC is expected to focus on the sustainable regional water resources management according to local differences, under the condition of ongoing climate change.

5. Conclusion

Based on daily data from 99 meteorological stations in SC during 1961–2016, growing season ET_0, as well as the spatiotemporal trends and the contribution of climate variable to ET_0 variation were analyzed. A change point for growing season ET_0 series was discovered in 1996 by the Cramer's test. Growing season ET_0 had demonstrated a significant decreasing trend ($P < 0.05$) from 1961 to 1996 by 10.25 mm/decade, while turned into a significantly increased trend ($P < 0.05$) from 1997 to 2016 by 8.12 mm/decade. In terms of spatial distribution, growing season ET_0 had an increasing trend from west to east whilst from north to south in SC. For climatic variables, T_{min}, T_{max} and RH were higher in SB, GB and east of YGP, while SD and WS had a converse trend. Meanwhile, T_{max}, WS and RH had a weakly decreased trend and SD decreased significantly in SC before 1996, while increased trends appeared in T_{max}, WS and SD after 1996. T_{min} had increased trends during the whole study period in SC. Due to different geographical location and topographical features, the trends of climatic variables in four sub-regions differed.

The sensitivity of ET_0 to RH was negative, while its sensitivity to the other five climatic variables was positive. RH was the most sensitive climatic variable for ET_0, followed by SD, T_{max}, T_{min} and WS in SC. The monthly sensitivity coefficients of climatic variables varied during the growing season, and the sensitivity coefficients for climatic variables showed great differences in spatial distribution. Meanwhile, the sensitivity coefficient of ET_0 for the climatic variables was mutative with the climate change.

The monthly contribution of each variable to ET_0, determined by the sensitivity coefficient of climatic variable and the magnitude of its changing trend, were temporally unstable and varied considerably over the growing season. The proportional contributions of T_{max}, T_{min}, WS, RH, SD to the trend in ET_0 were −0.15, 0.15, −0.14, 0.03, −3.96% during the period 1961–1996, respectively. Therefore, SD was the main contributor to the change of growing season ET_0 in SC from 1961 to 1996. The proportional contributions of T_{max}, T_{min}, WS, RH, SD to the increased ET_0 were 0.63, 0.34, 0.74, 1.99, 0.49% during the period 1997–2016, respectively, inferring that RH was the dominant variable for the increase in ET_0 in SC.

The increase in ET_0 will result in higher water consumption for the

Table 6
Average crop water demand during growing season and trends of four sub-regions (WSP: Western-Sichuan Plateau; SB: Sichuan Basin; YGP: Yunnan-Guizhou Plateau; GB: Guangxi Basin) in Southwest China (SC).

Regions	Cropping systems	Multi-year average (mm)	1961–1996		1997–2016		1961–2016	
			Z	Slope	Z	Slope	Z	Slope
YGP	Rape-Rice	800	−2.77**	−1.134	2.04*	1.073	−1.79	−0.461
	Early rice-Late rice	828	−2.77**	−1.116	1.72	1.071	−1.59	−0.414
WSP	Highland barley	479	−0.18	−0.201	2.89**	1.763	−0.08	−0.046
GB	Early rice-Late rice	892	−3.07**	−1.935	0.36	1.058	−2.13*	−0.654
	Corn-Late rice	865	−2.98**	−1.889	0.42	1.005	−2.06*	−0.652
SB	Rape-Rice	779	−3.26**	−1.948	0.49	1.225	−2.54**	−0.773
	Wheat-Rice	750	−3.31**	−1.929	0.55	1.229	−2.62**	−0.791

* Indicates significance levels of 0.05.
** Indicates significance levels of 0.01.

growth of crops, especially for WSP and YGP, appeared to have experienced a more significant increase ($P < 0.05$) from 1997 to 2016, which indicating crops is more likely to be threatened by drought, especially for rainfed agriculture areas in SC.

Acknowledgments

We would like to thank the China Meteorological Administration for providing the data used in the present study. This work was also financially funded by the National Key Research and Development Program of China (2016YFC0400206), the National Natural Science Foundation of China (51779161, 51009101), and National Key Technologies R&D Program of China (No. 2015BAD24B01).

References

Allan, R.G., Pereira, L.S., Raes, D., Smith, M., 1998. Crop Evapotranspiration-guidelines for Computing Crop Water requirements-FAO Irrigation and Drainage Paper No 56. Rome, Italy. .

Bandyopadhyay, A., Bhadra, A., Raghuwanshi, N.S., Singh, R., 2009. Temporal trends in estimates of reference evapotranspiration over India. J. Hydrol. Eng. 14, 508–515.

Burn, D.H., Hesch, N.M., 2007. Trends in evaporation for the Canadian Prairies. J. Hydrol. 336, 61–73.

Cong, Z.T., Yang, D.W., Ni, G.H., 2009. Does evaporation paradox exist in China? Hydrol. Earth Syst. Sci. 13, 357–366.

Dinpashoh, Y., Jhajharia, D., Fakheri-Fard, A., Singh, V.P., Kahya, E., 2011. Trends in reference crop evapotranspiration over Iran. J. Hydrol. 399, 422–433.

Estevez, J., Gavilan, P., Berengena, J., 2009. Sensitivity analysis of a Penman-Monteith type equation to estimate reference evapotranspiration in southern Spain. Hydrol. Process. 23, 3342–3353.

Fan, Z.X., Thomas, A., 2013. Spatiotemporal variability of reference evapotranspiration and its contributing climatic factors in Yunnan Province, SW China, 1961–2004. Clim. Change. 116, 309–325.

Fan, J.L., Wu, L.F., Zhang, F.C., Xiang, Y.Z., Zheng, J., 2016. Climate change effects on reference crop evapotranspiration across different climatic zones of China during 1956–2015. J. Hydrol. 542, 923–937.

Feng, L., Li, T., Yu, W.D., 2014. Cause of severe droughts in Southwest China during 1951–2010. Clim. Dyn. 43, 2033–2042.

Feng, Y., Cui, N., Gong, D., Zhang, Q., Zhao, L., 2017a. Evaluation of random forests and generalized regression neural networks for daily reference evapotranspiration modelling. Agric. Water Manage. 193, 163–173.

Feng, Y., Cui, N.B., Zhao, L., Gong, D.Z., Zhang, K.D., 2017b. Spatiotemporal variation of reference evapotranspiration during 1954–2013 in Southwest China. Quat. Int. 441, 129–139.

Feng, Y., Jia, Y., Cui, N., Zhao, L., Li, C., Gong, D., 2017c. Calibration of Hargreaves model for reference evapotranspiration estimation in Sichuan basin of southwest China. Agric. Water Manage. 181, 1–9.

Feng, Y., Jia, Y., Zhang, Q.W., Gong, D.Z., Cui, N.B., 2018. National–scale assessment of pan evaporation models across different climatic zones of China. J. Hydrol. 564, 314–328.

Fu, G., Yu, J., Zhang, Y., Hu, S., Ouyang, R., Liu, W., 2010. Temporal variation of wind speed in China for 1961–2007. Theor. Appl. Climatol. 104, 313–324.

Gao, Y., Wang, Y.M., Cheng, A.F., Li, J.G., Liu, L., 2014. Spatial and temporal trend of potential evapotranspiration and related driving forces in Southwestern China, during 1961–2009. Quat. Int. 336, 127–144.

Gao, Z.D., He, J.S., Dong, K.B., Bian, X.D., Li, X., 2016. Sensitivity study of reference crop evapotranspiration during growing season in the West Liao River basin, China. Theor. Appl. Climatol. 124, 865–881.

Golubev, V.S., Lawrimore, J.H., Groisman, P.Y., Speranskaya, N.A., Zhuravin, S.A., Menne, M.J., Peterson, T.C., Malone, R.W., 2001. Evaporation changes over the contiguous United States and the former USSR: a reassessment. Geophys. Res. Lett. 28, 2665–2668.

Gong, L.B., Xu, C.Y., Chen, D.L., Halldin, S., Chen, Y.Q.D., 2006. Sensitivity of the Penman-Monteith reference evapotranspiration to key climatic variables in the Changjiang (Yangtze River) basin. J. Hydrol. 329, 620–629.

Grimenes, A.A., Thue-Hansen, V., 2006. The reduction of global radiation in south-eastern Norway during the last 50 years. Theor. Appl. Climatol. 85, 37–40.

Haktanir, T., Citakoglu, H., 2014. Trend, independence, stationarity, and homogeneity tests on maximum rainfall series of standard durations recorded in Turkey. J. Hydrol. Eng. 19 05014009.

Hupet, F., Vanclooster, M., 2001. Effect of the sampling frequency of meteorological variables on the estimation of the reference evapotranspiration. J. Hydrol. 243, 192–204.

IPCC, 2007. Climate Change 2007: the Physical Science Basis, Summary for Policymakers. Cambridge University Press, Cambridge 2007.

Jhajharia, D., Dinpashoh, Y., Kahya, E., Singh, V.P., Fakheri-Fard, A., 2012. Trends in reference evapotranspiration in the humid region of northeast India. Hydrol. Process. 26, 421–435.

Ji, Y., Zhou, G., 2011. Important factors governing the incompatible trends of annual pan evaporation: evidence from a small scale region. Clim. Change. 106, 303–314.

Jiang, S.Z., Yang, R.Y., Cui, N.B., Zhao, L., Liang, C., 2018. Analysis of drought vulnerability characteristics and risk assessment based on information distribution and diffusion in Southwest China. Atmosphere 9, 239.

Kang, S., Gu, B., Du, T., Zhang, J., 2003. Crop coefficient and ratio of transpiration to evapotranspiration of winter wheat and maize in a semi-humid region. Agric. Water Manage. 59, 239–254.

Lenhart, T., Eckhardt, K., Fohrer, N., Frede, H.G., 2002. Comparison of two different approaches of sensitivity analysis. Phys. Chem. Earth. 27, 645–654.

Li, Z., Zheng, F.L., Liu, W.Z., 2012. Spatiotemporal characteristics of reference evapotranspiration during 1961–2009 and its projected changes during 2011–2099 on the Loess Plateau of China. Agric. For. Meteorol. 154, 147–155.

Li, Z., Chen, Y.N., Yang, J., Wang, Y., 2014a. Potential evapotranspiration and its attribution over the past 50 years in the arid region of Northwest China. Hydrol. Process. 28, 1025–1031.

Li, Z.X., Feng, Q., Wei, L., Wang, T.T., Gao, Y., Wang, Y.M., Cheng, A.F., Li, J.G., Liu, L., 2014b. Spatial and temporal trend of potential evapotranspiration and related driving forces in Southwestern China, during 1961–2009. Quat. Int. 336, 127–144.

Li, B., Chen, F., Guo, H.D., 2015. Regional complexity in trends of potential evapotranspiration and its driving factors in the Upper Mekong River Basin. Quat. Int. 380, 83–94.

Li, Y.Z., Liang, K., Bai, P., Feng, A.Q., Liu, L.F., Dong, G.T., 2016. The spatiotemporal variation of reference evapotranspiration and the contribution of its climatic factors in the Loess Plateau, China. Environ. Earth Sci. 75, 354.

Li, C., Wu, P.T., Li, X.L., Zhou, T.W., Sun, S.K., Wang, Y.B., Luan, X.B., Yu, X., 2017. Spatial and temporal evolution of climatic factors and its impacts on potential evapotranspiration in Loess Plateau of Northern Shaanxi, China. Sci. Total Environ. 589, 165–172.

Liu, J.G., Li, S.X., Ouyang, Z.Y., Tam, C., Chen, X.D., 2008. Ecological and socioeconomic effects of China's policies for ecosystem services. PNAS 105, 9477–9482.

Liu, C.M., Liu, X.M., Zheng, H.X., Zeng, Y., 2010. Change of the solar radiation and its causes in the Haihe River Basin and surrounding areas. J. Geogr. Sci. 20, 569–580.

Liu, X.M., Luo, Y.Z., Zhang, D., Zhang, M.H., Liu, C.M., 2011. Recent changes in pan-evaporation dynamics in China. Geophys. Res. Lett. 38, L13404.

Liu, T.G., Li, L.G., Lai, J.B., Liu, C., Zhuang, W.H., 2016. Reference evapotranspiration change and its sensitivity to climate variables in southwest China. Theor. Appl. Climatol. 125, 499–508.

Liu, Z.C., Lu, G.H., He, H., Wu, Z.Y., He, J., 2017. Understanding atmospheric anomalies associated with seasonal pluvial-drought processes using Southwest China as an example. J. Geophys. Res. Atmos. 122, 12210–12225.

Liu, B.J., Chen, X.H., Li, Y., Chen, X.H., 2018. Long-term change of potential evapotranspiration over southwest China and teleconnections with large-scale climate anomalies. Int. J. Climatol. 38, 1964–1975.

Liu, X.M., Zhang, D., 2013. Trend analysis of reference evapotranspiration in Northwest China: the roles of changing wind speed and surface air temperature. Hydrol. Process. 27, 3941–3948.

McVicar, T.R., Rodercik, M.L., Donohue, R.J., Li, L.T., Van Niel, T.G., Thomas, A., Grieser, J., Jhajharia, D., 2012. Global review and synthesis of trends in observed terrestrial near-surface wind speeds: implications for evaporation. J. Hydrol. 416, 182–205.

Moonen, A.C., Ercoli, L., Mariotti, M., Masoni, A., 2002. Climate change in Italy indicated by agrometeorological indices over 122 years. Agric. For. Meteorol. 111, 13–27.

Mushtaq, S., Dawe, D., Lin, H., Moya, P., 2006. An assessment of the role of ponds in the adoption of water-saving irrigation practices in the Zhanghe Irrigation System. China. Agric. Water Manage. 83, 100–110.

Najafi, M.R., Zwiers, F.W., Gillett, N.P., 2015. Attribution of arctic temperature change to greenhouse-gas and aerosol influences. Nat. Clim. Chang. 5, 246–249.

Nyakudya, I.W., Stroosnijder, L., 2014. Effect of rooting depth, plant density and planting date on maize (Zea mays L.) yield and water use efficiency in semi-arid Zimbabwe: Modelling with Aqua Crop. Agric. Water Manage. 146, 280–296.

Ørum, J.E., Boesen, M.V., Jovanovic, Z., Pedersen, S.M., 2010. Farmers' incentives to save water with new irrigation systems and water taxation-A case study of Serbian potato production. Agric. Water Manage. 98, 465–471.

Pachauri, R.K., Allen, M.R., Barros, V.R., Broome, J., Cramer, W., Christ, R., Church, J.A., Clarke, L., Dahe, Q., Dasgupta, P., 2014. Climate Change 2014: Synthesis Report. Contribution of Working Groups I, II and III to the Fifth Assessment Report of the Intergovernmental Panel on Climate Change.

Papaioannou, G., Kitsara, G., Athanasatos, S., 2011. Impact of global dimming and brightening on reference evapotranspiration in Greece. Geophys. Res-Space Phys. 116, D09107.

Pérez-Sarmiento, F., Mirás-Avalos, J.M., Alcobendas, R., Alarcón, J.J., Mounzer, O., Nicolas, E., 2016. Effects of regulated deficit irrigation on physiology, yield and fruit quality in apricot trees under Mediterranean conditions. Span. J. Agric. Res. 1–12.

Peterson, T.C., Golubev, V.S., Groisman, P.Y., 1995. Evaporation losing its strength. Nature 377, 687–688.

Qian, Y., Wang, W.G., Leung, L.R., Kaiser, D.P., 2007. Variability of solar radiation under cloud-free skies in China: the role of aerosols. Geophys. Res. Lett. 34, L12804.

Qian, Y., Kaiser, D.P., Leung, L.R., Xu, M., 2015. More frequent cloud-free sky and less surface solar radiation in China from 1955 to 2000. Geophys. Res. Lett. 33, 311–330.

Roderick, M.L., Hobbins, M.T., Farquhar, G.D., 2009. Pan evaporation trends and the terrestrial water balance: II. Energy balance and interpretation. Geogr. Compass. 3, 761–780.

Ruelland, D., Ardoin-Bardin, S., Billen, G., Servat, E., 2008. Sensitivity of a lumped and semi-distributed hydrological model to several methods of rainfall interpolation on a large basin in West Africa. J. Hydrol. 361, 96–117.

Shadmani, M., Marofi, S., Poknian, M., 2012. Trend analysis in reference evapotranspiration using mann-kendall and Spearman's rho tests in arid regions of Iran. Water Resour. Manag. 26, 211–224.

Shi, Z.J., Xu, L.H., Yang, X.H., Guo, H., Dong, L.S., Song, A.Y., Zhang, X., Shan, N., 2017.

Trends in reference evapotranspiration and its attribution over the past 50 years in the Loess Plateau, China: implications for ecological projects and agricultural production. Stoch. Environ. Res. Risk Assess. 31, 257–273.
Stanhill, G., Cohen, S., 2001. Global dimming: a review of the evidence for a widespread and significant reduction in global radiation with discussion of its probable causes and possible agricultural consequences. Agric. For. Meteoro. 107, 255–278.
Stocker, T., Qin, D., Plattner, G.K., Tignor, M., Allen, S.K., Boschung, J., Nauels, A., Xia, Y., Bex, V., Midgley, P.M., 2014. Climate Change 2013: The Physical Science Basis. Cambridge University Press, Cambridge, UK and New York, NY.
Streets, D.G., Yu, C., Wu, Y., Chin, M., Zhao, Z., Hayasaka, T., Shi, G., 2008. Aerosol trends over China, 1980–2000. Atmos. Res. 88, 174–182.
Tang, B., Tong, L., Kang, S.Z., Zhang, L., 2011. Impacts of climate variability on reference evapotranspiration over 58 years in the Haihe river basin of north China. Agric. Water Manage. 98, 1660–1670.
Tang, B., Tong, L., Kang, S.Z., 2013. Effects of spatial station density and interpolation methods on accuracy of reference crop evapotranspiration. Trans. Chin. Soc. Agric. Eng. 29 (13), 60–66 (in Chinese).
Thomas, A., 2008. Agricultural irrigation demand under present and future climate scenarios in China. Glob. Planet. Change 60, 306–326.
Tong, L., Kang, S.Z., Zhang, L., 2007. Temporal and spatial variations of evapotranspiration for spring wheat in the Shiyang river basin in northwest China. Agric. Water Manage. 87, 241–250.
Türkeş, M., 1996. Spatial and temporal analysis of annual rainfall variations in Turkey. Int. J. Climatol. 16, 1057–1076.
Wang, Y., Jiang, T., Bothe, O., Fraedrich, K., 2007. Changes of pan evaporation and reference evapotranspiration in the Yangtze River basin. Theor. Appl. Climatol. 90, 13–23.
Wang, Z.L., Xie, P.W., Lai, C.G., Chen, X.H., Wu, X.S., Zeng, Z.Y., Li, J., 2017. Spatiotemporal variability of reference evapotranspiration and contributing climatic factors in China during 1961–2013. J. Hydrol. 544, 97–108.
Xu, M., Chang, C.P., Fu, C., Qi, Y., Robock, A., Robinson, D., Zhang, H., 2006. Steady decline of east Asian monsoon winds, 1969–2000: evidence from direct ground measurements of wind speed. J. Geophys. Res.-Atmos. 111, D24111.
Yan, G.X., Wu, Z.Y., Li, D.H., 2013. Comprehensive analysis of the persistent drought events in Southwest China. Disaster Adv. 6, 306–315.
Ye, X., Li, X., Liu, J., Xu, C., Zhang, Q., 2014. Variation of reference evapotranspiration and its contributing climatic factors in the Poyang Lake catchment, China. Hydrol. Process. 28, 6151–6162.
Yin, Y.H., Wu, S.H., Dai, E.F., 2010. Determining factors in potential evapotranspiration changes over China in the period 1971–2008. Chin. Sci. Bull. 55, 3329–3337.
Zhang, Y.Q., Liu, C.M., Tang, Y.H., Yang, Y.H., 2007. Trends in pan evaporation and reference and actual evapotranspiration across the Tibetan Plateau. J. Geophys. Res. Atmos. 112 D12110.
Zhang, X.Q., Ren, Y., Yin, Z.Y., Lin, Z.Y., Zheng, D., 2009. Spatial and temporal variation patterns of reference evapotranspiration across the Qinghai–Tibetan Plateau during 1971–2004. J. Geophys. Res.-Atmos. 114, D15105.
Zhang, D., Liu, X.M., Hong, H.Y., 2013. Assessing the effect of climate change on reference evapotranspiration in China. Stoch. Environ. Res. Risk Assess. 27, 1871–1881.
Zhang, K.X., Pan, S.M., Zhang, W., Xu, Y.H., Gao, L.G., Hao, Y.P., Wang, W., 2015. Influence of climate change on reference evapotranspiration and aridity index and their temporal-spatial variations in the Yellow River Basin, China, from 1961 to 2012. Quat. Int. 380, 75–82.
Zhao, L.L., Xia, J., Sobkowiak, L., Li, Z.L., 2014. Climatic characteristics of reference evapotranspiration in the hai river basin and their attribution. Water 6, 1482–1499.
Zuo, D.P., Xu, Z.X., Yang, H., Liu, X.C., 2012. Spatiotemporal variations and abrupt changes of potential evapotranspiration and its sensitivity to key meteorological variables in the Wei River basin, China. Hydrol. Process. 26, 1149–1160.